A FAST KALMAN FILTER FOR TIME-LAPSE ELECTRICAL RESISTIVITY TOMOGRAPHY

Arvind K. Saibaba, Eric L. Miller

Tufts University
Dept. of Electrical and Computer Engineering

Peter K. Kitandis

Stanford University
Dept. of Civil and Environmental Engineering

ABSTRACT

We present a reduced complexity algorithm for time-lapse Electrical Resistivity Tomography (ERT) based on an extended Kalman filter. The key idea of the fast algorithm is an efficient representation of state covariance matrix at each step as a weighted combination of the system noise covariance matrix and a low-rank perturbation term. We propose an efficient algorithm for updating the weights and the basis of the low-rank perturbation. The overall computational cost at each iteration is $\mathcal{O}(Nn_m)$ and storage cost $\mathcal{O}(N)$, where N is the number of grid points, and n_m is the number of measurements . The performance of this algorithm is demonstrated on a challenging application of monitoring the CO_2 plume using synthetic ERT data.

Index Terms— Extended Kalman Filter, Electrical Resistivity Tomography, Fast algorithms

1. INTRODUCTION

Because the electrical conductivity and permittivity of the earth vary with geophysical and hydrological properties such as salinity, porosity, and saturation, electrical resistance tomography (ERT) has proven to be a useful method for imaging dynamic processes in the subsurface with applications including carbon sequestration [2], and contaminant remediation [1], among others. Accurate reconstruction using ERT is very challenging because of the diffusive nature of the underlying physics, as well as application-dictated limitations in the manner in which data can be collected. These challenges are only exacerbated by modern data acquisition systems capable of collecting information at rates up to every three hours over several days. To address these issues here we propose a computationally efficient method for time lapse ERT using a fast Extended Kalman filter. We demonstrate the utility of the approach in the context of a problem where we seek to track the movement of CO_2 in the subsurface, to provide a reliable tool for geological carbon dioxide sequestration.

Kalman filtering is a fundamental tool in statistical time series analysis used to estimate the state of dynamical systems for which partial, noisy observations are available. Dominated by the need to store and invert $N \times N$ state covariance matrix where N is the dimension of the state variable, the standard implementations of the Kalman filter are $\mathcal{O}(N^2)$ in memory and $\mathcal{O}(N^3)$ in computational cost. For the problem of interest here the state vector contains the degrees of freedom of a 3D finite difference or finite element model of tracer concentration throughout the subsurface so that N is quite large, on the order of 10^6. For such large problem sizes and with high frequency of data acquisition, the cost of the standard implementation is prohibitively expensive.

In this paper, we will focus our attention on the case in which the state dynamics are provided by a random walk forecast model. This model is useful in practical applications in which data is acquired at a rapid rate and when changes in subsequent states are small and can approximated by a random process. This model has previously been applied for filtering in the context of electrical impedance tomography [3], electrical resistivity tomography [5] and CO_2 monitoring using seismic travel-time tomography [4]. In our approach, we consider an efficient representation of the posterior covariance matrix as a low-rank perturbation of the system noise covariance matrix. The system noise covariance matrix Γ_{prior} is modeled as the inverse of a discrete differential operator and updates to the weights and the bases are calculated efficiently by solving a generalized eigenvalue problem and repeated application of the Sherman-Morrison-Woodbury update. The resulting algorithm for the Kalman filter with Random walk forecast model scales as $\mathcal{O}(N)$, both in memory and computational cost. For a small number of measurements, this procedure can be made numerically exact. However, as the number of measurements increase, for several choices of measurement operators and noise covariance matrices, the spectrum of the generalized Hermitian eigenvalue problem decays rapidly and we are justified in only retaining the dominant eigenmodes. We discuss tradeoffs between accuracy and computational cost.

The resulting algorithms are applied to a synthetic application to continuously track CO_2 plume in the subsurface using time-lapse ERT. The significant reduction in computational costs make it more feasible for real-time data assimilation by providing accurate estimate of the quantity that is being imaged and also reliable estimates of uncertainty.

2. PROBLEM FORMULATION

We consider a synthetic setup for time-lapse ERT to monitor CO_2 plume in an aquifer. ERT yields voltage measurements in response to series of known input currents. The currents and voltages ϕ are related electrical conductivity $\sigma(\mathbf{x})$ of the subsurface via the Poisson's equation

$$-\nabla \cdot (\sigma \nabla \phi) = I\left(\delta(\mathbf{x}-\mathbf{x}_+) - \delta(\mathbf{x}-\mathbf{x}_-)\right)$$

where $\mathbf{x}_+$ and $\mathbf{x}_-$ refer to the injection and extraction locations of the electric current of strength I. Absorbing boundary conditions are chosen to model a semi-infinite domain [1]. We assume the relationship between the concentration $s(\mathbf{x},t)$ of the CO_2 with the conductivity $\sigma(\mathbf{x},t)$ as $\sigma(\mathbf{x},t) = \sigma_0 + \beta c(\mathbf{x},t)$, where σ_0 is the background conductivity. In this paper we only consider the simple linear case but extensions to other petrophysical relations based on Archie's law are possible [7]. ERT data was then synthetically generated using a known configuration of electrodes that remains fixed throughout the injection experiment. This data is then used to reconstruct and monitor the CO_2 plume in the domain.

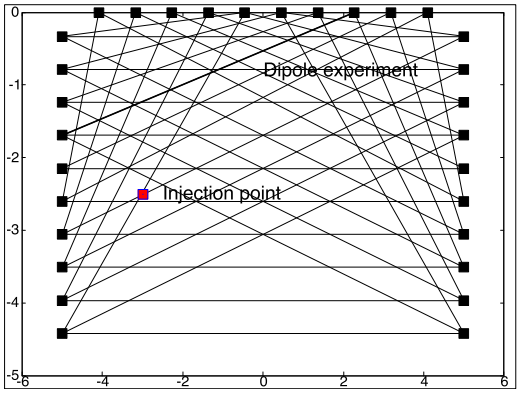

Fig. 1. Setup of measurement acquisition geometry indicating the dipole locations and the injection point of the CO_2 plume

We denote, by s_k and y_k the state variable (representing conductivity) and observations (electrical potential) at step k. We assume that s_k and y_k satisfy the following dynamical system

$$\begin{aligned} s_{k+1} &= F_k s_k + w_k & w_k &\sim \mathcal{N}(0, \Gamma_{\text{prior}}) \\ y_{k+1} &= h(s_{k+1}) + v_k & v_k &\sim \mathcal{N}(0, \Gamma_{\text{noise}}). \end{aligned}$$

The system noise w_k is modeled as a Gaussian process with zero mean and covariance Γ_{prior}. Further, h, the *measurement operator*, represents the nonlinear mapping induced by Poisson's equation between the electrical conductivity to the measurements. In a typical ERT application, multiple source dipoles located within the subsurface as well as on the surface are employed. For each source, the potential is measured over a discrete set of locations. The setup of the measurement acquisition is displayed in Figure 1. In total $n_s = 30$ sensors are placed in the periphery of the domain and $n_e = 40$ experiments are carried out by picking 2 sensors as a dipole and collecting measurements at all other sensor locations in an alternating fashion. The dipoles are chosen in a cross-medium configuration in order to make the data more sensitive in the center of the domain. With this configuration, the total number of measurements collected at any time step is $n_m = n_e(n_s - 2) = 1120$ measurements. The vector y_k represents the data from all sources at all locations collected at time k and are assumed to be corrupted by noise, here modeled as $\mathcal{N}(0, \Gamma_{\text{noise}})$. Under the random walk model, the state transition matrix F_k is taken as the identity matrix, i.e. $F_k = I$. This model is useful in practical applications in which data is acquired at a rapid rate and when changes in subsequent states are small.

3. FAST EXTENDED KALMAN FILTER

In this work, we will assume that $\Gamma_{\text{prior}}^{-1}$ is modeled as a discrete representation of a differential operator, for example the Laplacian, and acts as a spatial regularization to encourage smoothness. Note that in our implementation we do not compute the entries of Γ_{prior} explicitly; rather the matrix-vector products $\Gamma_{\text{prior}}x$ and $\Gamma_{\text{prior}}^{-1}x$ computed using a sparse LU methods are sufficient. As a result storage costs of Γ_{prior} are $\mathcal{O}(N)$. The entries of Γ_{prior} can also be represented by Matérn covariance kernels which specify two-point spatial correlations and the resulting dense matrices can be efficiently represented using Hierarchical matrix techniques in $\mathcal{O}(N)$ or $\mathcal{O}(N \log N)$ [9].

The Kalman filter is often written out in two stages [9]: 1) the prediction stage, in which the state estimate at the previous time-step is used to produce an estimate of the state at the current time step, and 2) the update stage, in which the prediction is combined with the observation to refine the state estimate. The nonlinearity in the measurement process can be handled by linearizing about the current state estimate, $h(s_{k+1}) \approx h(s_k) + H_k(s_{k+1} - s_k)$,where, $H_k = \frac{\partial h}{\partial s}\big|_{s_k}$ (computing using the adjoint state method [1]). This is known as the Extended Kalman Filter. Let $\hat{s}_{k_2|k_1}$ and $\Sigma_{k_2|k_1}$ denote the estimate and covariance (respectively) at step k_2 given information till step k_1. The equations for the Kalman filter can be summarized as

$$\begin{aligned} \Sigma_{k+1|k+1} &= \left[(\Sigma_{k|k} + \Gamma_{\text{prior}})^{-1} + H_k^T \Gamma_{\text{noise}}^{-1} H_k\right]^{-1} \\ \hat{s}_{k+1|k+1} &= \Sigma_{k+1|k+1}\left[(\Sigma_{k|k} + \Gamma_{\text{prior}})^{-1}\hat{s}_{k|k} \right. \\ &\qquad \left. + H_k^T \Gamma_{\text{noise}}^{-1}(y_{k+1} - h(\hat{s}_{k|k}) - H_k \hat{s}_{k|k})\right] \end{aligned}$$

However, a naive implementation of the algorithm scales as $\mathcal{O}(N^3)$. This cost is prohibitively expensive for finely discretized grids. We take a different approach: the key idea of our algorithm is an efficient representation of the covariance matrix $\Sigma_{k|k}$ as a weighted combination of the system

covariance matrix Γ_{prior} and a low-rank perturbative term. This can be written as $\Sigma_{k|k} = \alpha_k \Gamma_{\text{prior}} - W_k D_k W_k^T$. Here, $W_k^T \Gamma_{\text{prior}}^{-1} W_k = I$. The update to the coefficients α_k, diagonal matrix D_k and the low-rank basis W_k can be achieved efficiently at a cost $\mathcal{O}(N n_m + n_m^3 + r_k^2 N)$, where r_k is the rank of the matrix W_k and equal to the number of columns. The procedure is summarized in algorithm 1.

The low-rank perturbative matrix W_k contains information about the dominant eigenmodes of the generalized eigenvalue problem (GEP) $H_k^T \Gamma_{\text{noise}}^{-1} H_k w = \lambda \Gamma_{\text{prior}}^{-1} w$. There is strong theoretical and numerical evidence that the spectrum of the GEP defined above decays rapidly (see also section 4) and therefore we are justified in retaining only the dominant modes. These modes combine information from the system noise and the data misfit Hessian. When the measurement operator H_k is constant at all time-steps, the eigendecomposition needs be to computed only once and can be done offline. The dominant eigenmodes are computed using an efficient randomized approach developed in [8]. Another valuable component in this algorithm is the truncation of the rank of the rank of the addition of two low-rank terms in step 7 of algorithm 1. The rank of the low-rank perturbation is controlled by the parameter tol and the details are provided in [9].

Algorithm 1 Fast Extended Kalman Filter for random walk forecast model [9]

1: **for** $k = 1, \ldots, N_t$ **do**
2: $\alpha_{k+1} = \alpha_k + 1$ and $\bar{D}_k = \alpha_{k+1}^{-1}(\alpha_{k+1} I - D_k)^{-1} D_k$
3: Compute the Jacobian $H_k = \frac{\partial h}{\partial s}\big|_{s_k}$
4: Compute the generalized eigendecomposition

$$H_k^T \Gamma_{\text{noise}}^{-1} H_k = \Gamma_{\text{prior}}^{-1} U_k \Lambda_k U_k^T \Gamma_{\text{prior}}^{-1}$$

where, $U_k^T \Gamma_{\text{prior}}^{-1} U_k = I$.
5: Compute $F_k = \alpha_{k+1} \Gamma_{\text{prior}} H_k^T - W_k D_k (W_k^T H_k)$
6: Compute $\hat{s}_{k+1|k} = \hat{s}_{k|k} + F_k (H_k F_k + \Gamma_{\text{noise}})^{-1} \left(y_k - h(\hat{s}_{k|k})\right)$.
7: $[W_{k+1}, \hat{D}] = \text{AddLowRank}\left(W_k, \bar{D}_k, U_k, \Lambda_k, \Gamma_{\text{prior}}^{-1}\right)$
8: $D_{k+1} \overset{\text{def}}{=} \alpha_{k+1}(I + \alpha_{k+1}^{-1} \hat{D}^{-1})^{-1}$
9: **end for**

The efficient representation of $\Sigma_{k|k}$ at each time step has other advantages as well. Useful uncertainty measures such as variance (computed as the diagonals of $\Sigma_{k|k}$), entropy (and relative entropy) of the distribution $\mathcal{N}(\hat{s}_{k|k}, \Sigma_{k|k})$ can be computed efficiently as a consequence of this representation. Another way to visualize the uncertainty is by drawing samples from the distribution $\mathcal{N}(\hat{s}_{k|k}, \Sigma_{k|k})$. This can be efficiently computed without explicitly factorizing the matrices $\Sigma_{k|k}$ but by propagating realizations taken from Γ_{prior} at a small additional cost. For lack of space, we do not discuss this further. The reader is referred to [9] for further details.

4. NUMERICAL EXPERIMENTS

The domain under consideration is a rectangular region of size $[-5, 5] \times [0, -5]\ m^2$. As the true CO_2 field to be recovered, we consider the exact analytic solution

$$c(\mathbf{x}; t) = \frac{5}{4\pi t \beta \sqrt{D_l D_t}} \exp\left(-\frac{(x - x_c(t))^2}{2 D_l t} - \frac{(y - y_c(t))^2}{2 D_t t}\right) [Kg/m^2]$$

where, $x_c(t) = -3 + u_x t$ [m] and $y_c(t) = -2.5$ [m]. This represents a Gaussian pulse injected at location $(-5, -2.5)$ [m] and is undergoing dispersion in the medium, advected with velocity $u_x = 2.5$ [m/hr]. Here, $D_l = 0.17[m^2/\text{hr}]$ and $D_t = 0.08[m^2/\text{hr}]$ are the lateral and transverse dispersivities, respectively. We take $\sigma_0 = 0.1[S/m]$ and $\beta = 0.2 Sm^2/Kg$Measurements are collected in 30 time intervals. For the system noise matrix Γ_{prior} we choose $\Gamma_{\text{prior}}^{-1} = L + \gamma I$, where, L is the 2D discrete Laplacian with Neumann b.c.s. and $\gamma = 10$. The noise covariance matrix is chosen to be $\sigma^2 I$, where $\sigma = 7 \times 10^{-3}$. Gaussian noise of 1% was added to the data. The grid size was $N = 50 \times 40 = 2000$. Results from larger grids will be reported in the poster.

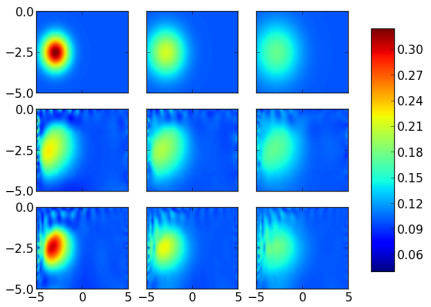

Fig. 2. Comparison of the reconstruction using the full EKF and the fast algorithm proposed in section 3 at time steps $10, 20$ and 30 (top row) true state (middle row) reconstruction using fast algorithm with tol$= 10^{-3}$ and (bottom row) reconstruction using full EKF

We now report the numerical results of the reconstruction using the full EKF that is computationally more expensive and our fast algorithm that we proposed in Section 3. We truncate the low-rank perturbation by controlling the tolerance in Algorithm 1 to be tol $= 10^{-3}, 10^{-6}, 10^{-9}$. It can be seen from Figure 3 that the error due to the low-rank truncation is quite small and the error is comparable with the full extended Kalman filter which scales as $\mathcal{O}(N^3)$. The visual comparison between the true and the reconstructed field is provided in Figure 2 and is also quite good. Due to the initial error caused to rank truncation, and the subsequent error due linearization about the incorrect state, the truncated rank algorithm take some time steps before it reaches the same error as the full algorithm. In the absence of noise, the error

in the truncated rank algorithms decrease monotonically with decreasing tolerance, as we should expect.

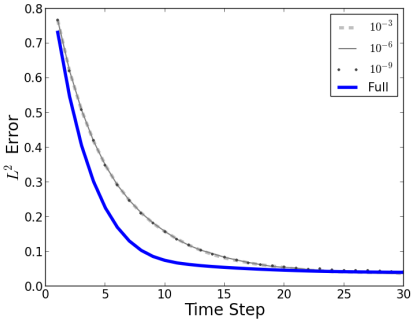

Fig. 3. The relative L^2 error of the reconstruction using full EKF and the fast algorithm for the extended Kalman filter with the effective rank of the perturbation truncated using a tolerance of tol $= 10^{-3}, 10^{-6}, 10^{-9}$

Without the low-rank truncation, the rank of the perturbation would grow linearly at each time step. At the end of 30 time steps, the total rank would have been $33,600$ and any computational gain due to this representation would have been completely lost. However, due to the effective rank-truncation strategy, the maximum rank of the perturbation term is at most 700 for the smallest tolerance used. It can also be seen that the effective rank grows in the initial time steps, due to the entry of information through the combined eigenmodes of the data and the prior. However, since the underlying parameter field that we would like to reconstruct changes very slowly relative to the rate of the measurement acquisition, the effective rank of the perturbation does not grow significantly and plateaus.

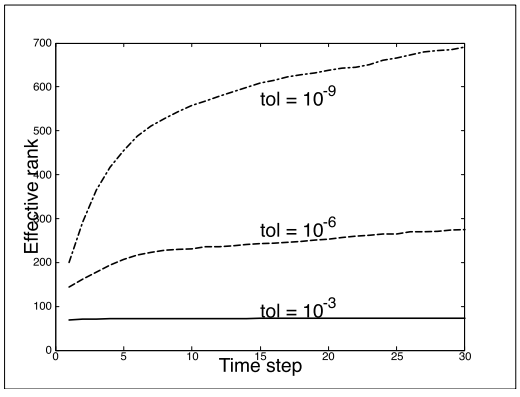

Fig. 4. Effective rank of the low-rank perturbative term in Section 3. Three different tolerances are use to truncate of the perturbative term, tol $= 10^{-3}, 10^{-6}, 10^{-9}$.

Further validation of our algorithm is necessary by comparing with data generated from a forward model that is more sophisticated than our crude analytical solution. Our algorithms are also widely applicable to a wide range of scenarios making it a viable candidate for real-time monitoring of dynamic processes whose state variables are of high-dimension.

Acknowledgment: We would like to thank Alireza Aghasi for kindly making his code ERT2D `http://users.ece.gatech.edu/aaghasi3/PDF%20Files/ERT2D.zip` available to us.

5. REFERENCES

[1] A. Aghasi, and E.L. Miller. Sensitivity calculations for Poisson's equation via the adjoint field method *GRSL*, 237-241, 2012, IEEE.

[2] C.R. Carrigan, X. Yang, D. LaBrecque, D. Larsen, and D. Freeman, A.L. Ramirez, W Daily, R. Aines, R. Newmark, J. Friedmann, and others Electrical resistance tomographic monitoring of CO_2 movement in deep geologic reservoirs *International Journal of Greenhouse Gas Control*, 2013, Elsevier.

[3] KY Kim, BS Kim, MC Kim, YJ Lee, and M Vauhkonen. Image reconstruction in time-varying electrical impedance tomography based on the extended Kalman filter. *Measurement Science and Technology*, 12(8):1032, 2001.

[4] Y.J. Li, S. Ambikasaran, E.F. Darve, and Kitanidis P.K. A Kalman filter powered by H-matrices for quasi-continuous data assimilation problems. *Submitted*, 2013.

[5] V. Nenna, A. Pidlisecky, and R. Knight. Application of an extended Kalman filter approach to inversion of time-lapse electrical resistivity imaging data for monitoring recharge. *Water Resources Research*, 47(10):W10525, 2011.

[6] E.A. Pnevmatikakis, K.R. Rad, J. Huggins, and L. Paninski. Fast Kalman filtering and forward-backward smoothing via a low-rank perturbative approach. *Journal of Computational and Graphical Statistics*, (just-accepted), 2013.

[7] D. Pollock, and O. Cirpka. Temporal moments in geoelectrical monitoring of salt tracer experiments. *Water Resources Research*, 2008.

[8] A.K. Saibaba and P.K. Kitanidis. Randomized square-root free algorithms for generalized hermitian eigenvalue problems. *ArXiv preprint http://arxiv.org/abs/1307.6885*.

[9] A.K. Saibaba and E.L. Miller and P.K. Kitanidis. Fast Kalman Filter using Hierarchical-matrices and low-rank perturbative approach *ArXiv preprint arXiv:1405.2276*.